Journal of Engineering Mathematics **46:** 299–312, 2003.

Thermomechanical behavior of a viscoelastic finite circular cylinder under harmonic deformations

V. G. KARNAUKHOV and I. K. SENCHENKOV
Timoshenko Institute of Mechanics, National Academy of Sciences of Ukraine, Nesterov Str., 3, Kiev 03057, Ukraine. e-mail:term@inmech.kiev.ua

Received 12 September 2002; accepted in revised form 4 March 2003

Abstract. A coupled thermomechanical behavior of a finite viscoelastic cylinder under harmonic kinematic excitation at its ends is investigated. The method of superposition is utilized to determine the stress-strain state of the cylinder. A refined asymptotic technique is developed to find the stress-strain state at each point of the body including the corner. Stiffness characteristics are examined over a broad range of cylinder-geometry parameters. By use of known stress components the function for the dissipation rate is constructed and the temperature field of vibration heating is calculated by solving the appropriate heat-conduction boundary-value problem. For the case of strong temperature dependence of loss modulus the phenomenon of thermal instability is examined.

Key words: coupled thermoviscoelasticity, finite cylinder, harmonic loading, method of superposition, thermal instability

1. Introduction

Cylindrical members are widely used in engineering applications. Therefore the static and dynamic behavior of a cylinder under mechanical and thermal loadings has been extensively studied in the past. Filon [1] used the Lamé method of superposition [2, Chapter 12] to investigate the stress state of an elastic finite cylinder. In [3–7] Lamé's method was further developed. In the papers cited the boundary-value problem was reduced to infinite systems of algebraic equations. Unfortunately, the approach developed does not provide an appropriate accuracy for the stress at the boundary surfaces. Essential difficulties arise in the case of a cylinder with clamped faces due to a stress singularity in the corner points. Grinchenko [8, Chapter 2] investigated the asymptotic behavior of infinite systems to improve a solution algorithm and to calculate the stress in all points of the cylinder, including the corner points.

The stress and strain as calculated can be used to investigate the self heating of a viscoelastic cylinder under cyclic compression. This problem is of great importance to many fields of engineering, where thermoplastic materials are widely used. A review of recent advances in the modeling of thermal failure and new results in the area is presented in [9, 10], where theoretical and experimental results are obtained for cylindrical specimens under kinematic harmonic excitation. Good agreement was found between the numerical and experimental temperatures for the PEBAX elastomer [9] and two commercial polymethylmethacrylate and polycarbonate specimens [10, 11] to cyclic compressive loading. The phenomenon of catastrophic failure due to self heating is a key problem in this context. It was established [9] that this scenario of self heating occurs if the loading parameter exceeds some critical value. Systematic investigations of the influence of coupling of mechanical and thermal fields

on stress-strain and thermal states are reported in [12, Chapters 7–8], [13, Chapter 6], [14, Chapter 8], [15].

The aim of our paper is to present the results of the investigation of stress-strain state and self heating of the viscoelastic finite cylinder under axial harmonic compression within a coupled problem of thermoviscoelasticity. The method of superposition is applied to calculate the distributions of stress and temperature [16]. Methods of calculation of critical loads are presented.

2. Statement of the problem

The axisymmetric stress-strain state of an isotropic linear viscoelastic cylinder (radius R, length H) is examined. The periodic variation in time of the axial component of the displacement is prescribed at the upper and lower faces of the cylinder. The lateral surface is traction-free.

It is assumed that a steady vibration problem is being considered; therefore, all field variables may be represented as follows:

$$\vec{u}(x,t) = \mathfrak{Re}\left\{\tilde{\vec{u}}(x)\mathrm{e}^{\mathrm{i}\omega t}\right\}, \ldots, \text{ etc},$$

where $\tilde{\vec{u}}$ is complex amplitude of the displacement, $\tilde{\vec{u}} = \vec{u}' + \mathrm{i}\vec{u}''$, ... ,etc; ω is the frequency of excitation, x represents the set of spatial coordinates and t is the time.

A cylindrical coordinate system ($Orz\varphi$) is introduced. The model is formulated starting from a notation in which all governing equations are expressed in complex variables [12, Chapters 7–8], [15], [17, Chapter 2]. When the cylindrical symmetry of the problem is taken into account, the equilibrium equations in cylindrical coordinates are:

$$\begin{aligned} &\frac{\partial\tilde{\sigma}_{rr}}{\partial r} + \frac{\tilde{\sigma}_{rr} - \tilde{\sigma}_{\varphi\varphi}}{r} + \frac{\partial\tilde{\sigma}_{rz}}{\partial z} = 0, \\ &\frac{\partial\tilde{\sigma}_{rz}}{\partial r} + \frac{1}{r}\tilde{\sigma}_{rz} + \frac{\partial\tilde{\sigma}_{zz}}{\partial z} = 0, \end{aligned} \tag{1}$$

where $\tilde{\sigma}_{mn}$ is the stress tensor for the complex amplitudes: $\tilde{\sigma}_{mn} = \sigma'_{mn} + \mathrm{i}\sigma''_{mn}$.

The effects of inertia and material nonlinearity are neglected. These points are discussed in [13, Chapter 8], [14, Chapter 9], [18–19].

Stress-strain constitutive relations may be written as

$$\tilde{\sigma}_{mn} = 2\tilde{G}(\tilde{\varepsilon}_{mn} + \frac{\tilde{\nu}}{1-2\tilde{\nu}}\tilde{\varepsilon}_{kk}\delta_{mn}), \tag{2}$$

where $\tilde{\varepsilon}_{mn}$ is the strain tensor for the complex amplitudes, $\tilde{G}$ and $\tilde{\nu}$ are the complex shear modulus and Poisson's ratio, respectively.

Boundary conditions are specified as follows:

$$\tilde{u}_z = \pm Ru_0, \quad \tilde{u}_r = 0 \quad \text{at } \zeta = \pm\zeta_0, \tag{3}$$

$$\tilde{\sigma}_{rr} = 0, \quad \tilde{\sigma}_{rz} = 0 \quad \text{at } \rho = 1. \tag{4}$$

The cylinder radius R is chosen as the characteristic dimension to define the dimensionless coordinates, so that $\rho = r/R$, $\zeta = z/R$ and $\zeta_0 = H/R$; Ru_0 is the amplitude of excitation.

Let us make some remarks. It is convenient to introduce the dimensionless stress $\hat{\sigma}_{mn} = \tilde{\sigma}_{mn}/2\tilde{G}$ into (1) and (2). Thereafter, if Poisson's ratio is supposed to be a real value $\tilde{\nu} = \nu$, the viscoelastic problem is reduced to a problem of elasticity. The applicability of this hypothesis was discussed in [20–23]. These findings provide an endorsement for the assumption $\tilde{\nu} = \nu$, particularly for bodies with a large free surface and for slightly compressible elastomers. States close to hydrostatic compression are sensitive to the volume deformation hypothesis. Such states occur in a compressed thin disk, (see for example [23]).

3. Construction of the solution

Following the superposition technique developed in [16], the displacements are expressed as

$$\begin{aligned}
\hat{u}_r = \frac{u_r}{R} &= 2(1-2\nu)\alpha_0\rho + \sum_{n=1}^{\infty}\{\alpha_n\left[4(1-\beta\nu)I_1(k_n\rho) - k_n\rho I_n(k_n\rho)\right] - \\
&\beta_n k_n I_1(k_n\rho)\}\cos\, k_n\varsigma + \sum_{i=1}^{\infty}(\gamma_i\lambda_i\varsigma\, \sinh\lambda_i\varsigma + \delta_i\lambda_i\varsigma\sinh\lambda_i\varsigma)\, J_1(\lambda_i\rho), \\
\hat{u}_z = \frac{u_z}{R} &= 2(1-2\nu)\gamma_0\rho + \sum_{n=1}^{\infty}\left[\alpha_n k_n\rho I_1(k_n\rho) + \beta_n k_n I_0(k_n\rho)\right]\sin k_n\varsigma + \\
&\sum_{i=1}^{\infty}\{\gamma_i\,[(3-4\nu)\,\sinh\,\lambda_i\varsigma - \delta_i\lambda_i\sinh\lambda_i\varsigma)]\}\, J_0(\lambda_i\rho),
\end{aligned} \tag{5}$$

where α_0, γ_0, α_n, β_n, γ_i, δ_i are arbitrary constants, $k_n = (2n-1)\pi/2\zeta_0$; λ_i are roots of the equation $J_1(\lambda) = 0$; J_0, J_1, I_0, I_1 are Bessel functions.

The expressions for the dimensionless stress are deduced from normalized constitutive relations (2)

$$\begin{aligned}
\hat{\sigma}_{rr} = {} & 2\alpha_0 + 2\nu\gamma_0 + \sum_{n=1}^{\infty}\{\alpha_n[-4(1-\nu)\frac{1}{\rho}I_1(k_n\rho) - k_n\rho I_1(k_n\rho) + \\
& (3-2\nu)k_n I_0(k_n\rho)] + \beta_n k_n[\frac{1}{\rho}I_1(k_n\rho) - k_n I_0(k_n\rho)]\}\cos k_n\varsigma - \\
& \sum_{i=1}^{\infty}(\gamma_i\lambda_i\varsigma\, \sinh\lambda_i\varsigma + \delta_i\lambda_i\cosh\lambda_i\varsigma)\frac{J_1(\lambda_i\rho)}{\rho} + \\
& \sum_{i=1}^{\infty}[\gamma_i(\lambda_i^2\varsigma\, \sinh\lambda_i\varsigma + 2\nu\lambda_i\cosh\lambda_i\varsigma) + \delta_i\lambda_i^2\cosh\lambda_i\varsigma]J_0(\lambda_i\rho); \\
\hat{\sigma}_{\varphi\varphi} = {} & 2\alpha_0 + 2\nu\gamma_0 + \sum_{n=1}^{\infty}\{\alpha_n[4(1-\nu)\frac{1}{\rho}I_1(k_n\rho) - (1-2\nu)k_n I_0(k_n\rho) \\
& -2\alpha_0 + 2\nu\gamma_0 + \beta_n k_n\frac{1}{\rho}I_1(k_n\rho)]\cos k_n\varsigma + \sum_{i=1}^{\infty}(\gamma_i\lambda_i\varsigma\, \sinh\lambda_i\varsigma + \delta_i\lambda_i\cosh\lambda_i\varsigma)\times \\
& \frac{J_1(\lambda_i\rho)}{\rho} + 2\nu\sum_{i=1}^{\infty}\gamma_i\lambda_i\cosh\lambda_i\varsigma)J_0(\lambda_i\rho);
\end{aligned}$$

$$\begin{aligned}
\hat{\sigma}_{zz} = {} & 4\nu\alpha_0 + 2(1-\nu)\gamma_0 + \sum_{n=1}^{\infty}\{\alpha_n[k_n^2\rho I_1(k_n\rho) + 2\nu k_n I_0(k_n\rho)] + \beta_n k_n^2 I_0(k_n\rho)\}\cos k_n\varsigma + \\
& \sum_{i=1}^{\infty}\{\gamma_i[-\lambda_i^2\varsigma\ \sinh\lambda_i\varsigma + 2(1-\nu)\lambda_i\cosh\lambda_i\varsigma] - \delta_i\lambda_i^2\cosh\lambda_i\varsigma\} \times J_0(\lambda_i\rho); \\
\hat{\sigma}_{rz} = {} & \sum_{n=1}^{\infty}\{\alpha_n k_n[-2(1-\nu)I_1(k_n\rho) + k_n\rho I_0(k_n\rho)] + \beta_n k_n^2 I_1(k_n\rho)\}\sin k_n\varsigma + \\
& \sum_{i=1}^{\infty}\{\gamma_i\lambda_i[\lambda_i\varsigma\ \cosh\lambda_i\varsigma - (1-2\nu)\sinh\lambda_i\varsigma] + \delta_i\lambda_i^2\sinh\lambda_i\varsigma]\} \times J_1(\lambda_i\rho).
\end{aligned} \tag{6}$$

Note that representations (5) and (6) formally give the possibility to satisfy all boundary conditions (3–4). We now proceed to find the unknown constants in Equations (6).

4. Analysis of the infinite system

Satisfying the homogeneous boundary conditions (3–4) for $\tilde{u}_r$ and $\tilde{\sigma}_{rr}$, we obtain the following relations between the coefficients:

$$\delta_j = -\gamma_j\zeta_0 th\lambda_j\zeta_0, \quad \beta_n k_n = -\alpha_n\big[k_n I_0(k_n)/I_1(k_n) - 2 + 2\nu\big]. \tag{7}$$

Then new coefficients x_n and y_j are introduced by the relations

$$\alpha_n = -\frac{(-1)^n x_n}{4k_n I_1(k_n)}, \quad \gamma_j = \frac{\zeta_0 y_j}{4\lambda_j J_0(\lambda_j)\cosh\lambda_j\zeta_0}. \tag{8}$$

Substituting the expressions for $\hat{u}_z$ and $\hat{\sigma}_{rr}$ in the remaining conditions (3–4), we obtain a system of two functional equations. To transform the system into algebraic form, the following Fourier-Bessel expansions are used:

$$\begin{aligned}
I_0(k_n\rho) &= 2\frac{I_1(k_n)}{k_n} + 2k_n I(k_n)\sum_{j=1}^{\infty}\frac{J_0(\lambda_j\rho)}{q_{nj}J_0(\lambda_j)}, \\
k_n\rho I_1(k_n\rho) &= 2I_0(k_n) - 4\frac{I_1(k_n)}{k_n} + 2k_n^2 I_0(k_n)\sum_{j=1}^{\infty}\frac{J_0(\lambda_j\rho)}{q_{nj}J_0(\lambda_j)} - 4k_n^3 I_1(k_n)\sum_{j=1}^{\infty}\frac{J_0(\lambda_j\rho)}{q_{nj}^2 J_0(\lambda_j)},
\end{aligned}$$

where $q_{nj} = k_n^2 + \lambda_j^2$.

As a result, after some transformations, we obtain the infinite system of algebraic equations

$$X_n t_n = \sum_{i=1}^{\infty} p_{ni} Y_i + \frac{4\nu}{\zeta_0 k_n^2}, Y_i s_i = \sum_{n=1}^{\infty} p_{ni} X_n, \tag{9}$$

where the following new unknowns are introduced:

$$X_n = \frac{x_n}{\gamma_0}, \quad Y_i = \frac{y_i}{\gamma_0}$$

and

$$\gamma_0 = \frac{u_0}{2(1-2\nu)\zeta_0 - \nu\sum_{n=1}^{\infty} X_n/k_n^2}; \quad p_{ni} = \frac{k_n^2}{q_{ni}^2} - \frac{1-\nu}{q_{ni}};$$

$$t_n = \frac{[k_n^2 + 2(1-\nu)]I_n^2(k_n) - k_n^2 I_0^2(k_n)}{4k_n^2 I_1^2(k_n)}; \; s_i = \frac{\zeta_o}{4}\left(\frac{3-4\nu}{\lambda_i}\tanh\,\lambda_i\zeta_0 - \frac{\zeta_0}{\cosh^2\,\lambda_i\zeta_0}\right).$$

As a consequence of the corner singularity, the series representing the stresses at the boundary surfaces converge very slowly. Nevertheless we can improve the numerical results sufficiently, using the asymptotics of the solution of the system (9). An efficient asymptotic technique was proposed in [16]. Following it, we express the principle terms of asymptotic representations of the unknowns in the system as

$$X_n = \frac{b}{k_n^\beta}; \quad Y_i = \frac{a}{\lambda_n^\alpha}. \tag{10}$$

Retaining only the principal terms in the system (9), we obtain the equations

$$\begin{aligned} -\frac{b}{4}\frac{1}{k_n^{\beta+1}} &= \frac{a}{k_n^{\alpha+1}}\left(\frac{1+\alpha}{4\sin\frac{1-\alpha}{2}\pi} - \frac{1-\nu}{2\sin\frac{1-\alpha}{2}\pi}\right); \\ \frac{3-4\nu}{4}\frac{a}{\lambda_i^{\alpha+1}} &= \frac{b}{\lambda_i^{\beta+1}}\left(\frac{1-\beta}{4\sin\frac{1-\beta}{2}\pi} - \frac{1-\nu}{2\sin\frac{1-\beta}{2}\pi}\right). \end{aligned} \tag{11}$$

The following summation rule is utilized:

$$\lim_{k\to\infty}\sum_{n=1}^{\infty}\frac{1}{k}f\left(\frac{n}{k}\right) = \int_0^{\infty} f(x)\mathrm{d}x.$$

It follows from Equations (11) that $\alpha = \beta$. The condition for the existence of a nonzero solution for the constants a and b leads to a transcendental equation for α, namely,

$$(3-4\nu)\sin^2\frac{1-\alpha}{2}\pi = [\alpha - (1-2\nu)][\alpha + (1-2\nu)]. \tag{12}$$

It has two real roots, one positive and one negative, both smaller than unity. The negative root is inconsistent with the assumptions leading to Equation (12) and should, therefore, be discarded. The method of reduction improves substantially if, in the course of transition to a finite system with M unknown X_n and N unknown Y_i, one lets

$$Y_i = \frac{Y_N\lambda_N^\alpha}{\lambda_i^\alpha}\;(i \geqslant N); \quad X_n = \frac{X_M k_M^\alpha}{k_n^\alpha}\;(n \geqslant M). \tag{13}$$

The infinite system (9) then becomes

$$X_n t_n = \sum_{i=1}^{N} p_{ni}Y_i + Y_N\lambda_N^\alpha\sum_{i=N+1}^{\infty}\frac{p_{ni}}{\lambda_i^\alpha} + \frac{4\nu}{\zeta_0 k_n^2}, Y_i s_i = \sum_{n=1}^{\infty} p_{ni}X_n + X_M k_M^\alpha\sum_{n=M+1}^{\infty}\frac{p_{ni}}{k_n^\alpha}, \tag{14}$$
$$(n = 1, 2, \ldots, M; \quad i = 1, 2, \ldots, N).$$

The criterion for selecting the number of unknowns M and N is the accuracy of the approximation by Fourier-Bessel series with a $(1-\rho)^{\alpha-1}$ type singularity for $\rho \to 1$; boundary conditions are, in this case, automatically satisfied within sufficient accuracy.

5. Calculation of the stresses

Having solved system (14) and inserted the values of the coefficients of X_n and Y_i into the expressions for displacements and stresses, we obtain the solution of our problem. A simple asymptotic analysis of these series indicates, however, that the stress series converge very slowly at the boundary surfaces. Since difficulties of such a nature are common to all stresses, we will illustrate the problem by giving a thorough analysis of the radial stress. We consider separately the cylindrical and the laminar components. The cylindrical component (series in n), marked by superscript "c", converges fast when $\rho < 1$, but as $\sum_{n=1}^{\infty} \frac{(-1)^n}{k_n^\alpha} \cos k_n \zeta$ when $\rho = 1$.

With the series expansion

$$\sum_{n=1}^{\infty} \frac{(-1)^n}{k_n^\alpha} \cos k_n \zeta \underset{\zeta \to \zeta_0}{\to} \frac{\zeta_0}{n} \Gamma(1-\alpha)(\zeta_0 - \zeta)^{\alpha-1} \cos \frac{1-\alpha}{2}\pi,$$

$$2^\alpha \pi \Gamma(\alpha) \sum_{n=1}^{\infty} \frac{\sqrt{n}}{(\pi n)^\alpha} J_{\alpha+\frac{1}{2}}(\pi n) \sin \frac{\pi n z}{h} = \sqrt{2}\frac{z}{h}\left(1 - \frac{z^2}{h^2}\right)^{\alpha-1}, \tag{15}$$

its convergence improved by Kummer's method, we obtain for $\rho = 1$

$$\begin{aligned} \hat{\sigma}_{rr}^c = & -\frac{\gamma_0}{4} \sum_{n=1}^{M} (-1)^n \left\{ X_n \left[k_n \frac{I_0^2(k_n)}{I_1^2(k_n)} - k_n - \frac{2(1-\nu)}{k_n} \right] - \frac{X_M k_M^\alpha}{k_n^\alpha} \right\} \times \\ & \cos k_n \zeta - \frac{X_M k_M^\alpha \gamma_0}{4} Z_1(\zeta), \end{aligned} \tag{16}$$

where

$$\begin{aligned} Z_1(\zeta) = & \sum_{n=1}^{\infty} \frac{(-1)^n \cos k_n \zeta}{k_n^\alpha} = -\frac{(\zeta_0^2 - \zeta^2)^{\alpha-1}}{2^\alpha \zeta_0^{\alpha-2} \Gamma(\alpha) \sin \frac{\alpha\pi}{2}} + \\ & \sum_{n=1}^{\infty} \left[\frac{(-1)^n}{k_n^\alpha} + \sqrt{\frac{k_n \pi \zeta_0}{2}} \frac{I_{n-\frac{1}{2}}}{k_n^2 \sin \frac{\alpha\pi}{2}} \right] \cos k_n \zeta. \end{aligned} \tag{17}$$

For the laminar component (series in j), marked by superscript 'l', at $\zeta = \zeta_0$ we have, analogously,

$$\hat{\sigma}_{rr}^l = \frac{\nu \zeta_0 \gamma_0}{2} \sum_{i=1}^{N} \left(Y_i - \frac{Y_N \lambda_N^\alpha}{\lambda_i^\alpha} \right) \frac{J_0(\lambda_i \rho)}{J_0(\lambda_i)} + \frac{\nu \zeta_0 \gamma_0}{2} Y_N \lambda_N^\alpha Z_2(\rho), \tag{18}$$

where

$$\begin{aligned} Z_2(\rho) = & \sum_{i=1}^{\infty} \frac{1}{\lambda_i^\alpha} \frac{J_0(\lambda_i \rho)}{J_0(\lambda_i)} = \frac{(1-\rho^2)^{\alpha-1}}{2^\alpha \Gamma(\alpha) \cos \frac{\pi\alpha}{2}} - \frac{1}{2^\alpha \Gamma(\alpha+1) \cos \frac{\alpha\pi}{2}} + \\ & \sum_{i=1}^{\infty} \left[1 - \frac{J_0(\lambda_i)}{\cos \frac{\alpha\pi}{2} J_0(\lambda_i)} \right] \frac{1}{\lambda_i^\alpha} \frac{J_0(\lambda_i \rho)}{J_0(\lambda_i)}. \end{aligned} \tag{19}$$

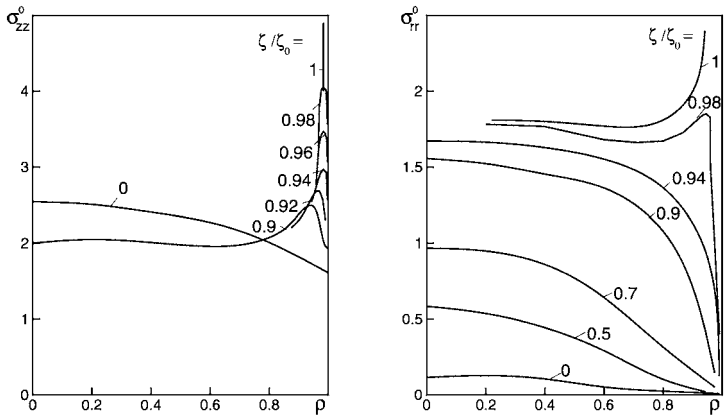

Figure 1. Distributions of normalized stress components σ^0_{zz} and σ^0_{rr} for some fixed values of ζ.

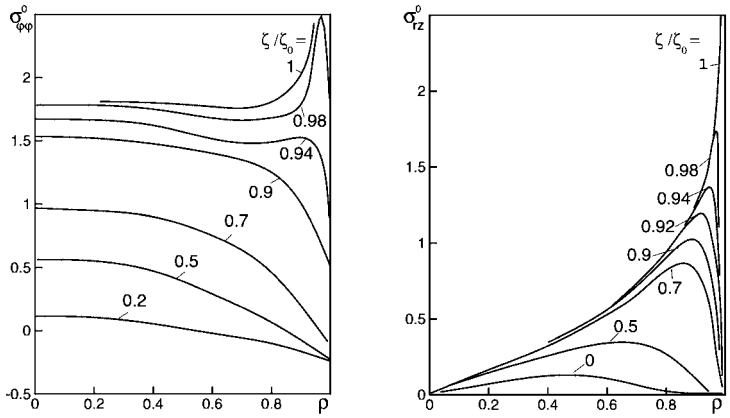

Figure 2. Distributions of normalized stress components $\sigma^0_{\varphi\varphi}$ and σ^0_{rz} for some fixed values of ζ.

The series in expressions (16–19) converge sufficiently fast. Expressions (17) and (19) indicate that the singularity found in the components of the stress tensor upon approaching a corner is of the same type as the singularity in the problem for quarter of plane in elasticity. With the solution given here, it is possible to calculate the stress-strain state at any point of a viscoelastic cylinder within any prescribed accuracy. Numerical values of the components of stress tensor, with $\nu = 0{\cdot}5$ and various fixed values of ζ, are shown in Figures 1 and 2. The graphs reflect the basic singularities' characteristics of such stresses. Normalized stresses are introduced as $\sigma^0_{\alpha\beta} = \hat{\sigma}_{\alpha\beta}/\varepsilon_0$, $\varepsilon_0 = Ru_0/H = u_0/\zeta_0$, $\alpha, \beta = r, \varphi, z$.

The stress distributions over the cylinder end faces are shown in Figure 3 for $\nu = 0{\cdot}4$ and $0{\cdot}5$. The indices of respective stresses are given here in parentheses. It is evident here that the stresses begin to increase fast when approaching a corner point and that, furthermore, the stress level rises appreciably with increasing Poisson ratio. We note that, when $\nu = 0{\cdot}5$, the state of a cylinder end face is 'hydrostatic' ($\sigma_{rr} = \sigma_{\varphi\varphi} = \sigma_{zz}$).

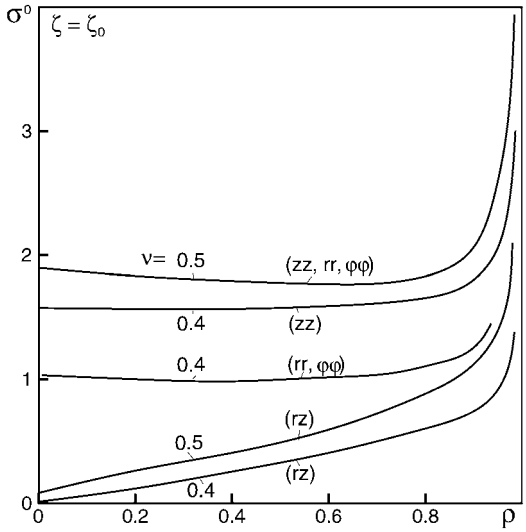

Figure 3. Stress distributions over the cylinder end for for $\nu = 0{\cdot}4$ and $\nu = 0{\cdot}5$.

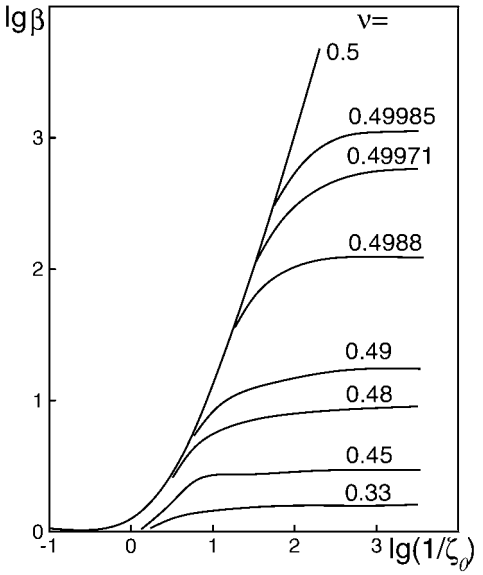

Figure 4. Dependence $\beta\ (\zeta_0)$ for fixed values of Poisson ratio.

6. Compression stiffness

Stiffness characteristics of the cylinder with clamped ends are of great practical importance for the design of rubber mounts for vibration proofing [14, Chapter 8], [24–25]. Let us define a stiffness coefficient as

$$\tilde{\beta} = \tilde{E}_{\text{eff}}/\tilde{E}. \tag{20}$$

Here $\tilde{E}_{\text{eff}}$ is an 'effective' complex modulus of axial compression of the mount

$$\tilde{E}_{\text{eff}} = \langle \tilde{\sigma}_{zz} \rangle / \varepsilon_0 = 2R^{-2} \int_0^R \tilde{\sigma}_{zz}(r, H) r \mathrm{d}r / (u_0 R/H) \tag{21}$$

and $\tilde{E}$ is the reference Young's modulus of material.

Obviously, $\tilde{\beta}$ is a real quantity $\tilde{\beta} = \beta$ when a Poisson's ratio $\tilde{\nu}$ is real. Using (6) and (21), we obtain

$$\beta = \frac{2\zeta_0(1-\nu)}{(1+\nu)[2(1-2\nu)\zeta_0 - \nu \sum_{n=1}^{n} X_n/k_n^2]}, \tag{22}$$

when the coefficients X_n are calculated from infinite system (9).

Numerical results are shown in Figures 4 and 5 as $\beta(\zeta_0)$ for a number of fixed ν values. The data in Figure 4 illustrate a very high sensitivity of stiffness to Poisson's ratio around $\nu = 0{\cdot}5$. It was shown in [14, Chapter 8] that the stiffness of a thin disk–like cylinder is determined by the volume modulus $\tilde{K}$

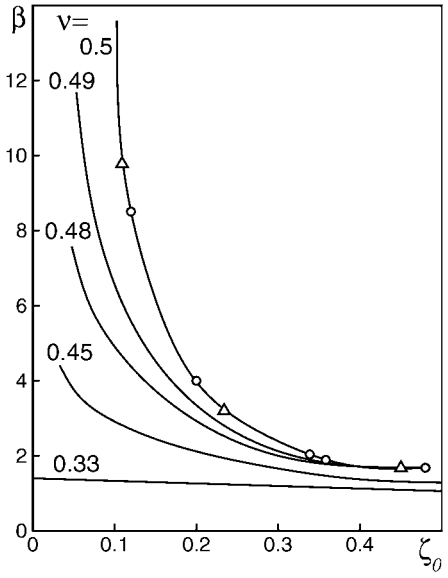

Figure 5. Dependence of β on geometry parameter ζ_0 for various Poisson ratios. Comparison with experimental data.

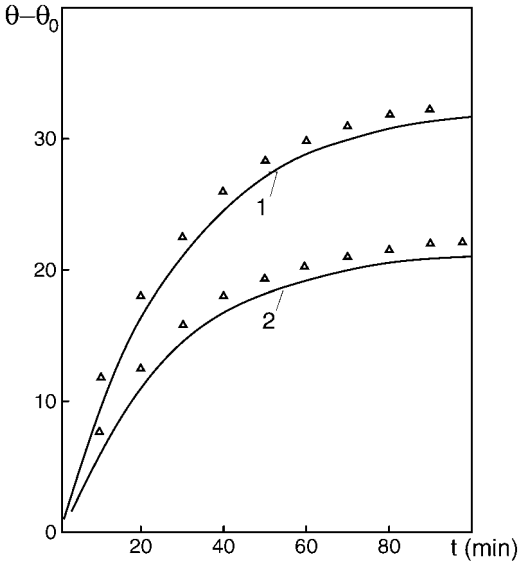

Figure 6. Temporal self-heating temperature curves in two points of rubber cylinder: $1 - \varphi = \zeta = 0$, $2 - \varphi = \zeta = 0{\cdot}5$. Comparison with experimental data.

$$\lim_{\zeta_0 \to 0} \beta = \frac{\tilde{K}}{\tilde{E}} = \frac{1-\nu}{(1+\nu)(1-2\nu)}.$$

For incompressible material the following asymptotic result is established for the case of ζ_0 vanishing to zero

$$\beta = \frac{1}{c\zeta_0^2} + O(\zeta_0),$$

when c is a certain coefficient independent of ζ_0.

The dependence of β on the geometry parameter ζ_0 for a number of fixed ν values is represented in Figure 5. Circles and triangles correspond to experimental data taken from [25]. The results presented show good agreement.

7. Vibration heating

Further attention is given to analysing the self heating in a cylinder sustaining a cyclic compressive loading. An important point of this part is to analyse the steady state resulting from the balance in the heat generation by the dissipation of part of the mechanical work and heat loss to the surroundings. The conditions of self-accelerating catastrophic-heating regime are discussed.

The evolution of the temperature θ is governed by the heat equation time-averaged over the cycle

$$c\frac{\partial \theta}{\partial t} = k\Delta\theta + \bar{D}, \tag{23}$$

where k is the heat-conductivity coefficient, c is the heat capacity per unit volume, $\bar{D}$ is the rate of calorific energy produced by dissipation per unit volume, $\Delta\theta$ is the Laplacian of the temperature.

Appropriate boundary and initial conditions are expressed as follows:

$$\begin{aligned} \theta &= \theta_0 \quad \text{at } |\zeta| = \pm\zeta_0 \text{ and } 0 < \rho < 1, \\ -\frac{\partial\theta}{\partial\rho} &= \gamma(\theta - \theta_0) \quad \text{at } \rho = 1 \text{ and } |\zeta| < \zeta_0, \\ \theta &= \theta_0 \quad \text{for } t = 0 \end{aligned} \tag{24}$$

where $\gamma = \alpha R/k$, α is a heat-transfer coefficient, θ_0 is the initial temperature.

The dissipated energy per unit volume is equal to the area of the hysteresis loop:

$$\bar{D} = \frac{\omega}{2\pi}\int_0^{2\pi/\omega} \sigma_{ij}\dot{\varepsilon}_{ij}\mathrm{d}t = \omega G''\left[\hat{\sigma}_{rr}^2 + \hat{\sigma}_{zz}^2 + \hat{\sigma}_{\varphi\varphi}^2 + 2\hat{\sigma}_{rz}^2 - \frac{\nu}{1+\nu}(\hat{\sigma}_{rr} + \hat{\sigma}_{zz} + \hat{\sigma}_{\varphi\varphi})^2\right], \tag{25}$$

where stress components $\hat{\sigma}_{ij}$ are defined by Equation (6); G'' is shear loss modulus.

It is remarkable that the dissipation function $\bar{D}$ is determined by dimensionless stress components which are calculated within the elastic statement of the mechanical problem. We note that according to Equations (17–18) the dissipation function has a singularity in the vicinity of a corner point: $\bar{D} \approx D_0[(1-\rho)^2 + (\zeta_0 - \zeta)^2]^{1-\alpha}$. Nevertheless, that singularity is integrable. So the temperature is a bounded function.

For the purpose of disigning structural components, it is useful to investigate the effects of the material parameters, as well as the effects of the loading parameters. Attention is devoted to a low carbon-filled rubber, a IRP 1347. According to Equation (25) the only viscoelastic property needed to characterize the dissipation function is the shear-loss modulus $G''(\omega, \theta)$. Typical experimental data for the IRP 1347 elastomer are fitted by the expression

$$G''(\omega, \theta) = G_0''(\omega)\exp[-0{\cdot}0143(\theta - 273)/\theta_r], \tag{26}$$

where θ_r is a reference temperature.

The following parameters values are used:

$$\begin{aligned} &R = 0{\cdot}05\ \mathrm{m}, \quad \zeta_0 = 0{\cdot}66, \quad \omega = 163{\cdot}71\ /\mathrm{s}, \quad \nu = 0{\cdot}5, \\ &\alpha = 10\ \mathrm{W/m^2K^\circ}, \quad \theta_r = 1\ \mathrm{K^\circ}, \quad \theta_0 = 293\ \mathrm{K^\circ}, \\ &k = 0{\cdot}22\ \mathrm{W/mK^\circ}, \quad c = 1{\cdot}86 \times 10^6\ \mathrm{J/m^3}, \quad G_0'' = 0{\cdot}863\ \mathrm{MPa}. \end{aligned} \tag{27}$$

The evolution of the temperature at two points of a cylinder with coordinates $\rho = \zeta = 0$ (curve 1) and $\rho = \zeta = 0{\cdot}5$ (curve 2) is represented in Figure 6. The loading parameter is $\varepsilon_0 = 3\%$. Triangles denote experimental results, whereas solid lines correspond to calculated data. As we can see, the discrepancy of theoretical and experimental results does not exceed 5%. The dependence of the maximum of the steady temperature on deformation ε_0 is shown in Figure 7. Curve 1 was calculated subject to the hypothesis $G'' = G''(\theta_0)$, where curve 2 was calculated using the temperature dependence (26). It is easy to recognize that, when $\varepsilon_0 \geqslant 2\%$, the range of the temperature rise is such that G'' cannot be considered as constant.

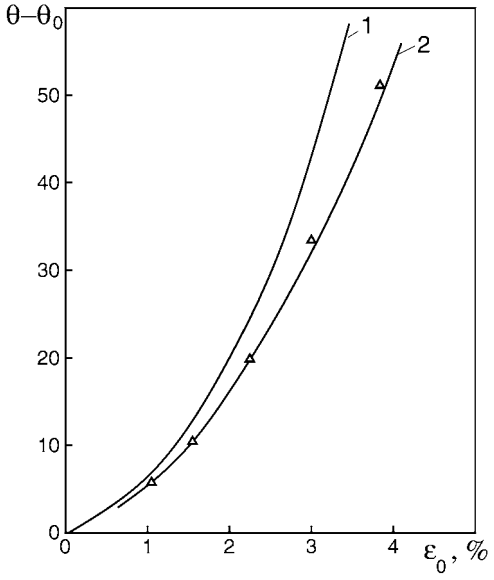

Figure 7. Dependence of maximum steady temperature in the rubber cylinder on reference deformation ε_0.

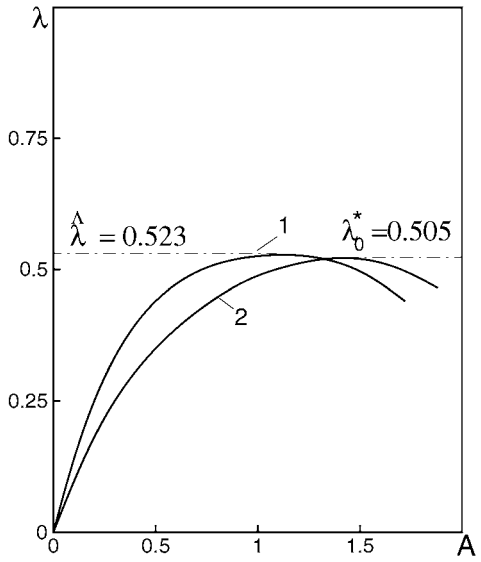

Figure 8. Dependence $\lambda(A)$ for eigenvalue problem. Curve 1 is calculated from (30) and curve 2 is obtained according to SAM.

8. Thermal instability

Catastrophic failure due to self heating is a common phenomenon in dissipative materials. This is particularly important for thermoplastics that have a very high temperature sensitivity and that can melt above a certain temperature. In earlier investigations [26, 27] it has been realized that the conditions of nonexistence of a steady-state solution have to be established to solve the problem. A material failure by thermal runaway necessarily appears in these cases. Below we analyse the existence of steady–state distributions of temperature in a cylinder made of linear viscoelastic material sustaining a compressive cyclic loading.

Let the temperature dependence of the loss modulus G'' be expressed as follows:

$$G''(\omega,\theta) = G_0''(\omega)\Phi[(\theta-\theta_0)/\theta_r], \tag{28}$$

where Φ is a certain function chosen to fit the experimental data.

The steady-state heat-conduction problem (23–24), with Equations (25) and (28) having been taken into account, is written as follows:

$$\Delta u + \lambda f(\rho,\zeta)\Phi(u) = 0, \frac{\partial u}{\partial n} + \chi u = 0 \quad \text{on } S, \tag{29}$$

where a dimensionless temperature u has been introduced, $u = (\theta-\theta_0)/\theta_r$; χ is a parameter of heat exchange, $\chi = \gamma/\theta_r$; λ is heat generation intensity parameter, $\lambda = \omega\varepsilon_0^2 G_0'' R^2/k\theta_r$; n is outer normal to S, and

$$f(\rho,\zeta) = {\sigma_{rr}^0}^2 + {\sigma_{zz}^0}^2 + {\sigma_{\varphi\varphi}^0}^2 + 2{\sigma_{rz}^0}^2 - \frac{\nu}{1+\nu}(\sigma_{rr}^0 + \sigma_{zz}^0 + \sigma_{\varphi\varphi}^0)^2.$$

The key question is to calculate the critical value λ^* of the intensity parameter λ, such that for $\lambda > \lambda^*$ there is no positive solution of problem (29) [26, 27].

In [26] for the bounded function $u/\Phi(u)$ is given as an upper estimate $\hat{\lambda}$ for λ^*. It is shown that

$$\hat{\lambda} = \mu_0 \max_{u \geqslant 0} \frac{u}{\Phi(u)}, \tag{30}$$

where μ_0 is the minimum eigenvalue of the associated linear problem

$$\Delta u + \mu f u = 0, \frac{\partial u}{\partial n} + \chi u = 0 \quad \text{on } S. \tag{31}$$

The function (30) gives a good estimate of the critical parameter λ^*. However, the method used to obtain Equation (30) does not allow to improve the result obtained. Moreover, this approach leads to a considerable error in the temperature distribution for $\lambda = \lambda^*$.

In [27] we propose two methods for solving of the problem (29) with a significantly nonlinear source $\Phi(u)$, which allow us to obtain the value of λ^* with any degree of accuracy.

Assuming that the function $u/\Phi(u)$ is bounded and that the estimate (30) is sufficiently exact, we propose the following approach to the solution of the system (29). Following the successive-approximation method (SAM), we write Equation (29) in the form

$$\Delta u + \mu g(x) u = g(x)[\mu u - \lambda \Phi(u)] \tag{32}$$

and solve the original nonlinear problem according to SAM. As a result the problem reduces to a sequence of linear boundary-value problems

$$\begin{aligned} &\Delta u_0 + \mu f u_0 = 0, \quad \frac{\partial u_0}{\partial n} + \chi u_0 = 0; \\ &\Delta u_n + \mu f u_n = f[\mu u_{n-1} - \lambda_{n-1} \Phi(u_{n-1})], \\ &\qquad \frac{\partial u_n}{\partial n} + \chi u_n = 0 \ (n = 1, 2, \ldots). \end{aligned} \tag{33}$$

It was shown in [27] that the initial approximation can be chosen as

$$\mu = \mu_0, \quad u_0 = A V_0(\rho, \zeta), \tag{34}$$

where $V_0(\rho, \zeta)$ is an orthonormalized eigenfunction corresponding to μ_0.

Substituting u_0 in (33) from the condition of the existence of the solution of boundary-value problems (33), we obtain the sequence

$$\lambda_{n-1} = \mu_0 A \left[\int_V f \Phi(u_{n-1}) u_0 dv \right]^{-1}. \tag{35}$$

The quantity $\lambda_n(A) \to \lambda(A)$ for $n \to \infty$. If the function $u/\Phi(u)$ is not bounded, the value of μ in (34) must be chosen in another way.

We consider specific examples of an investigation of the thermal instability of viscoelastic elements subjected to cyclic loading.

Problem (31) is solved by Galerkin's method for a cylinder characterized by data (27). For many viscoelastic materials, especially for highly filled elastomers, the function $\Phi(u) = \exp u$

provides a good approximation of the temperature dependence of the shear loss modulus. In Figure 8 the curves $\lambda(A)$ are represented for the problem defined by (33). Curve 1 is obtained based on Equation (30). Curve 2 is obtained based on a zero approximation (34). Both relations predict near values of the maximum λ, but a noticeable distinction of a critical temperature amplitudes A takes place.

So when $\lambda > \lambda^* = 0{\cdot}505$, a thermal steady state for the cylinder does not exist and an infinite temperature rise occurs.

9. Conclusions

The method of superposition is used as a direct and powerful technique to obtain the solution for an end-clamped finite cylinder. An asymptotic law for the Fourier coefficients allowed us to obtain accurate results for stress-strain fields everywhere, including corner points.

Next, the stiffness of a cylinder under axial compression has been investigated. A strong Poisson's ratio effect for a relatively thin disk has been established. Comparison of computational and experimental results was presented.

Once stress-strain field contributions were found, the rate dissipation function was calculated and the heat-conduction boundary-value problem defined. Then the evolution of the self-heating temperature for the cylinder was observed. Comparisons of computational and experimental results was given. In the case of strong temperature-dependent shear-loss modulus a phenomenon of thermal instability was examined. An approach for the calculation of critical values of the heat-intensity parameter has been developed.

Aknowledgements

The authors are greatly indebted to Dr. O. Chervinko and Dr. Y. Zhuk for their unfailing kindness in coming to our aid with suggestions, advice and useful help in the preparation of this paper.

References

1. L. N. G. Filon, On the elastic equilibrium of circular cylinders under certain practical systems of loads. *Phil. Trans. R. Soc. London A* 198 (1902) 147–233.
2. G. Lamé, *Lecons sur la Theorie Mathematique de l'Easticite des Corps Solides.* Paris: Bechelier (1852) 388 pp.
3. B. L. Abramjan, On problem of axisymmetric deformation of circular cylinder. *Dokl. Akad. Nauk Arm.SSR* 19 (1954) 3–12.
4. B. L. Abramjan, Some problems of equilibrium of circular cylinder. *Dokl. Akad. Nauk Arm.SSR* 26 (1958) 65–72.
5. B. L. Abramjan and A.A. Bablojan, On bend of thick circular plates under axisymmetrical load. *Izvestija Akad. Nauk Arm.SSR, Ser Phys.–Math.* 11 (1958) 95–106.
6. G. M. Valov, Axisymmetric problem on compression of elastic circular cylinder laying on smooth rigid foundation. *Izvestija Akad. Nauk SSSR. Mehanika i Mashinostroenie.* 6 (1961) 151–154.
7. K. Chandrashekhara, A note on the analysis of finite solid cylinder. *AIAA J.* 7 (1969) 1161–1163.
8. V. T. Grinchenko, *Equilibrium and Steady Vibrations of Elastic Bodies of Finite Size*. Kiev: Naukova Dumka (1978) 264 pp.
9. A. Molinary and Y. Germain, Self heating and thermal failure of polymers sustaining a compressive cyclic loading. *Int. J. Solids Struct*. 33 (1996) 3439–3462.

10. D. Rittel, An investigation of the heat, generated during cycling of two glassy polymers. Part 1: Experimental. *Mech. Mater.* 32 (2000) 137–147.
11. D. Rittel and Y. Rabin, An investigation of the heat, generated during cycling loading of two glassy polymers. Part II: Thermal analysis. *Mech. Mater.* 32 (2000) 149–159.
12. V. G. Karnaukhov, *Coupled Problems of Thermoviscoelasticity.* Kiev: Naukova Dumka (1982) 260 pp.
13. V. G. Karnaukhov, I. K. Senchenkov and B. P. Gumenjuk, *Thermomechanical Behavior of Viscoelastic Solids Under Harmonical Loading.* Kiev: Naukova Dumka (1985) 288 pp.
14. V. N. Poturaev, V. I. Dyrda, V. G. Karnaukhov *et al.*, *Thermomechanics of Elastomeric Structural Elements Under Cyclic Loading.* Kiev: Naukova Dumka (1985) 288 pp.
15. I. K. Senchenkov and V. G. Karnaukhov, Thermomechanical behavior of nonlinear viscoelastic materials under harmonic loading. *Int. Appl. Mech.* 37 (2001) 1400–1432.
16. V. T. Grinchenko, V. G. Karnaukhov and I. K. Senchenkov, Stress–strain state and heatup of viscoelastic cylinder with constraints at the ends. *Soviet Appl. Mech.* 11 (1975) 365–372.
17. R. M. Christensen, *Theory of Viscoelesticity. An Introduction.* New-York-London: Academic Press (1971) 338 pp.
18. Y. A. Zhuk, I. K. Senchenkov, V. I. Kozlov and G. A. Tabieva, Axisymmetric dynamic problem of coupled thermoviscoplasticity. *Int. Appl. Mech.* 37 (2001) 1211–1317.
19. Y. A. Zhuk, I. K. Senchenkov, G. A. Tabieva and O. P. Chervinko, Axisymmetric vibration and dissipative heating of a laminated inelastic disk. *Int. Appl. Mech.* 38 (2002) 95–102.
20. A. Johnson, Temperature field to thermomechanical coupling in a compressible viscoelastic sphere. *Acta Mechanica* 17 (1973) 201–209.
21. J. M. Lifshitz and H. Kolsky, The propagation of spherically divergent stress pulses in linear viscoelastic solids. *J. Mech. Phys. Solids.* 13 (1965) 361–376.
22. I. K. Senchenkov, Effect of dilatation loss on the vibration heating of hollow viscoelastic cylinders. *Soviet Appl. Mech.* 24 (1988) 788–793.
23. I. K. Senchenkov, O. P. Chervinko and V. I. Kozlov Energy analysis of the stress–strain state of a viscoelastic disk with rigidly fixed ends under cyclic compression . *Int. Appl. Mech.* 30 (1994) 791–796.
24. V. G. Karnaukhov and I. K. Senchenkov, Calculation of stiffness characteristics of cylindrical and prismatic shock absorber in compression and shear. *Mashinoved.* 3 (1976) 74–77.
25. S.D. Ponomarev, V.L. Biderman, K.K. Likharev *et al.*, *Calculation of Strength in Engineering, V2*. Moscow: GNTI (1958) 974 pp.
26. D. D. Joseph and E. M. Sparrow, Nonlinear diffusion induced by nonlinear sources. *Quart. Appl. Math.* 28 (1970) 327–341.
27. V. G. Karnaukhov and I. K. Senchenkov, Approximation methods for calculating critical thermal states. *Soviet Appl. Mech.* 12 (1976) 340–346.